

# INTEGRAL OBSERVATIONS OF GALAXY CLUSTERS

P. Goldoni<sup>1</sup>, A. Goldwurm<sup>1</sup>, P. Laurent<sup>1</sup>, M. Cassé<sup>2</sup>, J. Paul<sup>1</sup>, and C. Sarazin<sup>3</sup>

<sup>1</sup>DAPNIA/Service d'Astrophysique, CEA/Saclay, F-91191 Gif-Sur-Yvette, France

<sup>1</sup>IAP/Paris

<sup>2</sup>University of Virginia

## ABSTRACT

Cluster of galaxies are the largest concentrations of visible mass in the Universe and therefore a fundamental topic of cosmology and astrophysics. Recent radio, EUV, and X-ray observations suggest that clusters contain large populations of diffuse non-thermal relativistic and/or superthermal particles. These particles may be produced by acceleration in cluster merger shocks, AGNs, and/or supernovae in cluster galaxies. Models for the nonthermal populations in clusters indicate that they should produce substantial hard X-ray and  $\gamma$  luminosities. The possible role of nonthermal particles in the dynamics of clusters is one of the greatest uncertainties in their use as cosmological probes.

INTEGRAL offers, for the first time, the possibility of simultaneous medium resolution imaging ( $\sim 12$  arcmin) and high resolution spectroscopy ( $\Delta E/E \sim 2$  keV @ 1.3 MeV) with exceptional sensitivity in the hard X-ray/soft  $\gamma$ -ray band. The spatial resolution will allow discrete sources, such as AGNs, to be separated from the diffuse emission of the cluster. For nearby clusters, the spatial distribution of emission can be determined and compared to models for the nonthermal particle populations and observations in other wavebands. The spectral capabilities may allow different components of the nonthermal population to be detected separately. We present simulations of INTEGRAL observations of nearby galaxy clusters that show its capability for detecting the different phenomena responsible of clusters emission.

Key words: Clusters of Galaxies; imaging; Simulations.

## 1. INTRODUCTION

Clusters of Galaxies have been thoroughly investigated along the electromagnetic spectrum. Their properties give us valuable hints on the evolution of

the Universe and they are one of the best cosmological probes in our possession. Besides the thermal gas which dominates soft X-ray observations, it has long been believed that clusters of galaxies harbor a large populations of non thermal particles. Clusters should be effective traps for cosmic ray particles and the high temperature gas in the IntraCluster Medium (ICM) indicates that strong shock are operating inside it. If diffuse gas undergoes a strong shock, a portion of the shock energy goes into accelerating relativistic particles.

Relativistic electrons emit radiation either directly or by Inverse Compton interaction on the ambient photons. On the other hand relativistic protons collide on the nuclei in the intracluster medium producing radioactive isotopes and nuclear lines. The detection of diffuse *radio* halos in the cluster cores (see e.g. Giovannini et al. 1993) confirms this scenario.

Recently this topic has been revived by the detection of EUV and hard X-ray excesses (Bowyer et al. 1999, Sarazin & Lieu 1998, Fusco-Femiano et al. 1999, Rephaeli et al. 1999, Kaastra et al. 1998, Fusco-Femiano et al. 2000) in three nearby clusters: Coma, A2199 and A2256. The origin of this radiation has been widely discussed but no certain origin can be up to now determined (Sarazin 1999). The debate on the origin of hard X-ray excesses has been up to now hampered by the lack of imaging instruments in this energy domain.

Indeed at the flux level reported in the literature ( $\sim \text{few} \times 10^{-11}$  erg cm<sup>-2</sup> s<sup>-1</sup> in the 20-100 keV energy band, Bassani et al. 1999), there is a non negligible ( $\sim 10$  %) possibility of source confusion (mainly with AGNs) in the relatively large ( $\sim 1$  degree) field of view of actual instruments. Also the parameters and even the detection of the hard X-ray excess are highly dependent on the parameters of the spectral fit performed on the cluster soft X-ray emission.

The INTEGRAL satellite, the next ESA hard X-ray/soft  $\gamma$ -ray mission, will be able to advance our knowledge in these topics thanks to its exceptional sensitivity and imaging and spectral capabilities, unprecedented in this energy domain. The imaging ca-

pability of the IBIS imager will allow to identify the site of the emission and therefore the distribution of high energy electrons in the cluster. On the other hand the SPI spectrometer will allow to probe the acceleration of nuclei and their subsequent interaction with the ambient medium. We will show in the following the results of simulations of INTEGRAL observations which allow us to evaluate its impact on this problem.

## 2. THE INTEGRAL SATELLITE AND ITS INSTRUMENTS

INTEGRAL is a 15 keV-10 MeV  $\gamma$ -ray mission with concurrent source monitoring at X-rays (3-35 keV) and in the optical range (V, 500- 600 nm). All instruments are coaligned and have a large FOV, covering simultaneously a very broad range of sources. The INTEGRAL payload consists of two main  $\gamma$ -ray instruments, the spectrometer SPI and the imager IBIS, and of two monitor instruments, the X-ray monitor JEM-X and the Optical Monitoring Camera OMC.

The Imager on Board Integral Satellite (IBIS) provides diagnostic capabilities of fine imaging (12' FWHM), source identification and spectral sensitivity to both continuum and broad lines over a broad (15 keV-10 MeV) energy range. It has a continuum sensitivity of  $2 \cdot 10^{-7}$  ph cm $^{-2}$  s $^{-1}$  at 1 MeV for a  $10^6$  seconds observation and a spectral resolution better than 7 % @ 100 keV and of 6 % @ 1 MeV. The imaging capabilities of the IBIS are characterized by the coupling of its source discrimination capability (angular resolution 12' FWHM) with a field of view (FOV) of  $9^\circ \times 9^\circ$  fully coded,  $29^\circ \times 29^\circ$  partially coded FOV.

The spectrometer SPI will perform spectral analysis of  $\gamma$  ray point sources and extended regions with an unprecedented energy resolution of  $\sim 2$  keV (FWHM) at 1.3 MeV. Its large field of view ( $16^\circ$  circular) and limited angular resolution ( $2^\circ$  FWHM) are best suited for diffuse sources imaging but it retains nonetheless the capability of imaging point sources. It has a continuum sensitivity of  $7 \times 10^{-8}$  ph cm $^{-2}$  s $^{-1}$  at 1 MeV and a line sensitivity of  $5 \times 10^{-6}$  ph cm $^{-2}$  s $^{-1}$  at 1 MeV, both  $3\sigma$  for a  $10^6$  seconds observation.

The Joint European Monitor JEM-X supplements the main INTEGRAL instruments and provides images with 3' angular resolution in a  $4.8^\circ$  fully coded FOV in the 3-35 keV energy band. The Optical Monitoring Camera (OMC) will observe the prime targets of INTEGRAL main  $\gamma$  ray instruments. Its limiting magnitude is  $M_V \sim 19.7$  ( $3\sigma$ ,  $10^3$  s). The wide band observing opportunity offered by INTEGRAL provide for the first time the opportunity of simultaneous observing over 7 orders of magnitude.

All INTEGRAL instruments will be important in defining the emission from galaxy clusters, however

in this paper we will focus on IBIS contribution in defining the cluster shape at  $> 20$  keV energies and in identifying the origin of non thermal emission. We will show that IBIS will be able to determine the position of the  $> 20$  keV emission inside the cluster and therefore to give precious hints on the acceleration processes in the ICM.

## 3. SIMULATIONS

We simulated an IBIS  $10^6$  seconds observation of the Coma cluster, the pointings were centered on the cluster with a standard  $3 \times 3$  rectangular dithering pattern. SAX/PDS and RXTE observations of this cluster resulted in a detection of a 20-100 keV flux of about 2.2 mCrab in their  $1.3^\circ$  and  $1^\circ$  FWHM degree fields of view (Fusco-Femiano et al. 1999, Rephaeli et al., 1999). The origin of this emission is however unclear, as this kind of instrument is only capable of recording the *total* emission in the region without discriminating between the components. The spectral fit performed on the data required a non thermal component in excess of the thermal one. In Figure 1 we show a simulated spectrum of the 0.1-100 keV emission detected in Coma Cluster region by previous observations (Hughes et al. 1993, Rephaeli et al. 1999). The spectrum is the composition of a Raymond-Smith thermal model with  $kT = 9$  keV and a non thermal power law with photon index  $\alpha = 2.35$ .

Thermal emission clearly dominates the total flux at energies smaller than 50 keV. At higher energies however the emission is fainter and the situation is much less clear. From the plot it is evident that the parameters of the non thermal power law can be strongly influenced by a change in the parameters of the much stronger thermal component. Also a serendipitous AGN in the instrument FOV could substantially contribute to the total flux. The value of this component is difficult to assess as the spectral and temporal properties of AGNs are relatively unknown in this energy range. The strongest AGN in the Coma Cluster region is the Seyfert I galaxy X Comae (Bond & Sargent 1973), located  $\sim 30$  arcmin from the cluster centre. Extrapolating the ROSAT detection by Dow & White (1995) we have estimated a 20-60 keV X-ray flux of  $\sim 0.2$  mCrab.

We choose to simulate IBIS images of Coma cluster and X Comae in two energy bands: 20-60 keV ('thermal') and 40-120 keV ('non thermal'). Using the spectrum shown in Figure 1, the cluster emission in the low energy band is  $\sim 1.6$  mCrab, while in the high energy band is  $\sim 0.4$  mCrab. At low energies, we simulated its shape as a symmetric gaussian with 30' and 60' diameter FWHM, similar to what found in ROSAT images (see e.g. White et al. 1993). Our simulation assumes an isothermal cluster for simplicity, see Honda et al. 1996 for an analysis of Coma temperature structure. The non thermal emission structure is not determined, it should be linked

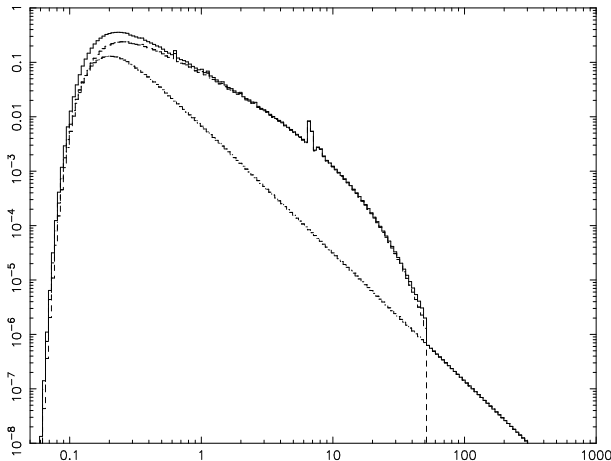


Figure 1. Simulated 0.1-100 keV spectrum of the Coma cluster region obtained using data from non imaging observations of Hughes et al. 1993 (GINGA) and Rephaeli et al. 1999 (RXTE). Two components are visible: the thermal Raymond-Smith model dominates at lower energy up to  $\sim 50$  keV while the non thermal power law only is present at higher energies

to clusters' radio halo whose radius varies with frequency. We consider that its dimensions should be somewhere in between the 30-40 arcmin radius at 150 MHz (Cordey 1985) and the  $\sim 10$  arcmin radius at 1.4 GHz (Kim et al. 1990). We simulated two non-thermal emission configurations: one gaussian with respectively 30' and 15' diameter FWHM. A smaller diameter being not resolvable by IBIS, it would result in a point source for the instrument. In the following we report the results of our simulations, we remark that the confidence level we report for our detections are preliminary.

Figure 2 and 3 show the result of our simulations in the 20-60 keV energy band, the cluster is clearly detected at a significance level of 20 and 60  $\sigma$  respectively while X Comae is detected in both cases at  $\sim 15 \sigma$  level. The cluster's extended nature is clearly visible in our images thus demonstrating IBIS' capabilities. The cluster appear in a much clearer way in Figure 3 due to the much higher surface brightness. A similar image will be the first at such energies and it will help determine the temperature structure of the cluster giving basic information on the distribution of  $>20$  keV gas in the cluster. Moreover it should be noted that the spectral analysis will not be hampered by the presence of a contaminating source which would be readily identified.

Figure 4 and Figure 5 show the result of our simulation in the 40-120 keV energy band in the two cases defined above. In both cases the cluster is detected but at a 5  $\sigma$  level in the first case and at a 10  $\sigma$  level in the second. Inspection of the image clearly shows that the cluster detection is much more difficult as surface brightness is much smaller in the second case. Background fluctuations could make the detection more difficult in this case, obliging to

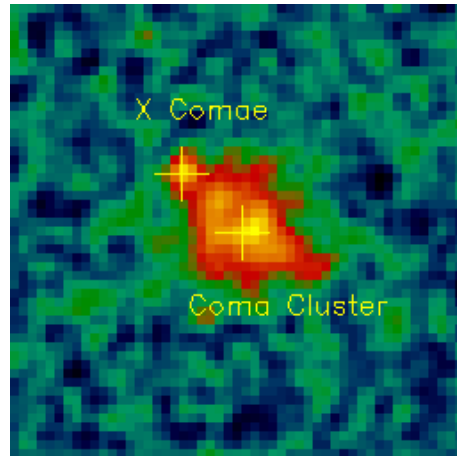


Figure 2. 20-60 keV color-coded image of a simulated  $10^6$  sec observation of the Coma cluster. X Comae flux is 0.2 mCrab while the cluster flux is 2.0 mCrab, its shape is a gaussian shape of 60' FWHM. The cluster is clearly visible as an extended source, and its shape its clearly distorted by the presence of X Comae on the upper left.

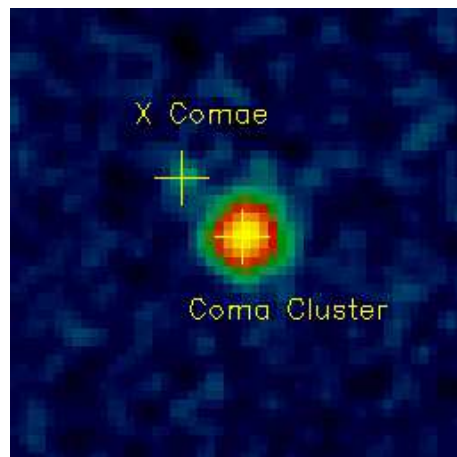


Figure 3. 20-60 keV color-coded image of a simulated  $10^6$  sec observation of the Coma cluster. Fluxes of sources are the same as above, the cluster is a gaussian of 30' FWHM. The cluster is again clearly visible as an extended source, while X Comae is a fainter source on the side which contributes a sizable flux.

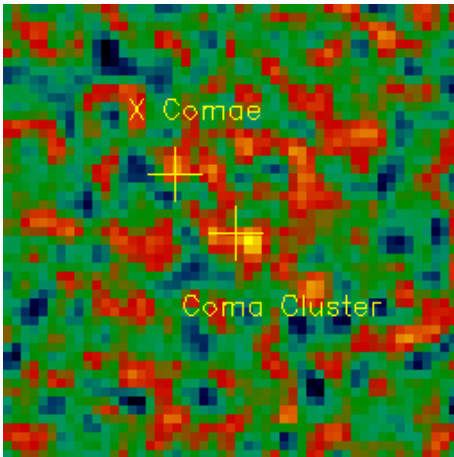


Figure 4. 40-120 keV color-coded image of a simulated  $10^6$  sec IBIS observation of the Coma cluster. The cluster has been simulated with a gaussian with 30' FWHM. The cluster is fainter and it is detected at a  $5 \sigma$  level. X Comae is proportionally stronger at a  $4 \sigma$  level.

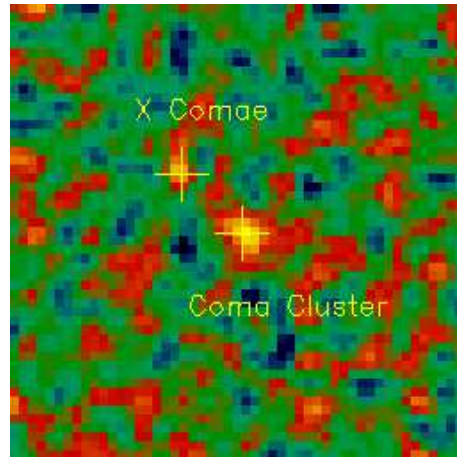


Figure 5. 40-120 keV color-coded image of a simulated  $10^6$  sec IBIS observation of the Coma cluster. The cluster has been simulated with a gaussian with 15' FWHM and is much more clearly visible than in Figure 4 as the flux is spreaded on a smaller surface. The detection significance is around  $\sim 10 \sigma$ . X Comae stays at  $4 \sigma$  level.

employ more sophisticated detection methods. As expected X Comae is proportionally stronger at a  $\sim 4 \sigma$  level.

#### 4. CONCLUSIONS

We simulated a  $10^6$  seconds observation of the Coma cluster with the IBIS instrument onboard the INTEGRAL satellite. We simulated a configuration comprising an AGN (X comae) in the Fully Coded Field of View of the instrument and we took the cluster emission parameter from Hughes et al. (1993) and Rephaeli et al. (1999). We demonstrated that IBIS is fully able to detect and separate the two components of the emission.

In the two images in the 20-60 keV energy band, the cluster is clearly detected as an *extended* source at a  $20\text{-}60\sigma$  level depending on the assumed shape. This will be the first image of the cluster at these energies and in itself will help better define the temperature distribution. Together with JEM-X data this should give a complete picture of the clusters' thermal emission.

At higher energies, in the 40-120 keV energy band, the results strongly depend from the unknown distribution of the clusters' non thermal emission. If its dimension is  $< 15$  arcminutes FWHM (600 kpc), then it can be detected at  $\sim 10 \sigma$  level. However if the emission is truly "diffuse" greater than IBIS resolving power, then the detection is much more difficult.

#### REFERENCES

- Bassani L. et al., 1999, Proceedings of 5th Compton Symposium Eds. M. L. Mc Connell, J.M. Ryan AIP Conference Proceedings
- Bond H.E. & Sargent W.L.W. 1973, ApJ 185, L109
- Bowyer S. et al. 1999, ApJ 526, 592
- Cordey R.A. 1985, MNRAS 215, 437
- Dow K.L. & White S.D.M. 1995, ApJ 439, 113
- Fusco-Femiano R. et al., 1999, ApJ 513, L24
- Fusco-Femiano R. et al., 2000, ApJ 534, L7
- Giovannini G. et al., 1993, ApJ 406, 399
- Honda H. et al. 1996, ApJ 473, L71
- Hughes J. et al. 1993, ApJ 404, 611
- Kaastra J.S. et al., 1998 Nucl. Phys. B 69, 567
- Kim K.T. et al., 1990, ApJ 355, 29
- Rephaeli, Y. et al., 1999, ApJ, 511 L21
- Sarazin C.L. & Lieu R. 1998 ApJ 494, L177
- Sarazin C.L. 1999 ApJ 520, 529
- White S.D.M. et al., 1993, MNRAS 261, L8